Available online at www.sciencedirect.com

SciVerse ScienceDirect

Ceramics International 38 (2012) 1181–1186

CERAMICS INTERNATIONAL

www.elsevier.com/locate/ceramint

Influence of vacant CeO_2 nanostructured ceramics on MgH_2 hydrogen desorption properties

Jelena Gulicovski, Željka Rašković-Lovre, Sandra Kurko, Radojka Vujasin, Zoran Jovanović, Ljiljana Matović, Jasmina Grbović Novaković *

Vinča Institute of Nuclear Sciences, Laboratory for Material Sciences, University of Belgrade, P.O. Box 522, Belgrade 11000, Serbia

Received 29 July 2011; received in revised form 30 July 2011; accepted 23 August 2011
Available online 1 September 2011

Abstract

The hydrogen desorption (HD) properties of MgH_2-CeO_2 composite prepared by mechanically milling of MgH_2 and cubic CeO_{2nano} have been examined. Morphology and microstructure of composites have been studied by X-ray powder diffraction (XRD), scanning electron microscopy (SEM), laser scattering analysis and correlated with desorption properties obtained by means of temperature programmed desorption (TPD). It has been shown that decrease of crystallite and particle size of the samples lead to significant lowering of desorption temperature. Further, the activation energy for desorption (E_A^{des}) has been calculated using Kissinger equation. Obtained value of 60 ± 10 kJ/mol indicates that the activation energy of hydrogen desorption is sufficiently decreased by the catalytic effect of vacant CeO_2 structure. Consequently the surface activation of sample plays a major role in HD reaction.

Keywords: A. Milling; B. Nanocomposites; D. CeO_2; Desorption properties; Hydrogen storage

1. Introduction

Among different materials for hydrogen storage, MgH_2 is one of the most promising material since of its high hydrogen capacity (7.6 wt.%), low cost, reversibility and high abundance. However, MgH_2 has high thermodynamic stability and slow hydrogen sorption kinetics. These disadvantages strongly limit its practical application. For the last decade, mechanical ball milling appeared as efficient way of MgH_2 structural destabilization [1]. The ball milling is well known method of mechanical deformation, which leads to reduction of particle and crystallite size and increase of specific surface area. On the other hand, great improvement was made by adding impurities and/or catalysts [1]. Sufficiently fast hydrogen sorption kinetics was achieved using metals, metal oxides, transition metal and transition metals oxides as additives [2–8].

Oelerich et al. investigated the influence of metal oxides on the sorption behavior of nanocrystalline Mg-based systems [2]. They found that the addition of oxides of the transition metals Ti, V, Cr, Mn and Fe, leads to significantly enhanced hydrogen desorption kinetics. The highest desorption rates were achieved with V_2O_5 and Fe_3O_4. Comparing to MgH_2–TM (TM – transition metals) composites, one can say that the metal oxides are dispersed more homogeneously in the material due to their brittleness and even in very small doses improves the desorption kinetics. The importance of the local electronic structure of catalysts was also pointed out [2,3]. From XANES spectra analysis of the MgH_2–TM oxide composites after ball milling, it was confirmed that the additives were reduced by MgH_2 to the metal oxides with lower oxidation states (+2 or +3) [4]. Therefore, the improvement of hydrogen sorption of MgH_2 occurs by the catalytic effect of the metal oxides, which has low oxidation state and the disarranged local structure. Bormann et al. proposed that oxide interfaces attached to the oxide catalysts might locally destabilize magnesium hydride phase [5]. The number of these oxide interfaces and their stability is determined by the type of the catalyst and the preparation method.

Shang and Guo reported a beneficial effect of $CeH_{2.35}$ for desorption kinetics in milled MgH_2–Ce mixture [6]. Interesting results were obtained for MgH_2 ball-milled with CeO_2 doped with 6 at.% of Pt [7]. The obtained hydrogen desorption rate in first 15 min was 5.2 wt.%. Authors reported that the addition of

* Corresponding author. Tel.: +381 11 3806552; fax: +381 11 3408224.
E-mail address: jasnag@vinca.rs (J. Grbović Novaković).

0272-8842/$36.00
doi:10.1016/j.ceramint.2011.08.047

non doped CeO_2 on MgH_2 appears to be irrelevant for desorption properties [7] while Song et al. reported the beneficial effect of CeO_2 on MgH_2 sorption kinetics [8].

As it can be seen a wide range of different metal oxides were used to improve the properties of MgH_2 as a hydrogen storage material. Despite the abundant literature on this subject, more research is needed in order to elucidate relative effects of particle size, presence of defects, grain boundaries, ternary magnesium–metal oxides, impurities, cycling, and so on. It has been unclear yet what the actual mechanism of catalysis for hydrogen sorption is; whether it is the influence of electronic structure, oxidation state, crystal structure of additives or formation of very high defect density on the surface of the powder particles. Understanding the factors involved in the dehydration reaction is necessary in order to gain influence on it.

In some papers, it was concluded that the rate-determining step of the hydrogen desorption (HD) reaction for pure MgH_2 was the nucleation and growth of Mg phase [9,10]. However, Hanada et al. modified the surface condition of the MgH_2 powder by Ni catalyst and HD reaction was significantly improved and transformed into a first-order one [11]. Since Mg has no strong catalytic effect for dissociation of H_2 molecule into H atoms on the surface, the recombination process on the MgH_2 surface should be taken into account as a rate determining step of the HD reaction for pure MgH_2 [12]. Hence, Hanada et al. proposed a new HD reaction model [11]. They assumed that the HD reaction from MgH_2 to $Mg + H_2$ follows a modified first-order reaction model, in which a surface condition is taken into account. As the surface condition, they introduce an activated surface area $1 - \theta(t)$ and a non-activated surface area $\theta(t)$ on the non-catalyzed MgH_2 powder, which are normalized by the total surface area. On the activated surface area, they assumed that hydrogen atoms are easily recombined into hydrogen molecules and then released. Furthermore, the non-activated surface area $\theta(t)$ is an exponential type decreasing function of reaction time as follows:

$$\theta(t) = \exp(1 - vt) \tag{1}$$

where v is a reaction rate constant. Thus, the activated surface area $1 - \theta(t)$ increases with time evolution and finally reaches 1. This assumption suggests that the recombination rate of H_2 on the surface gradually increases with the increasing time by a surface modification during the HD reaction.

If the HD reaction as a function of time is described by first order reaction, the activation energy can be determined by Kissinger method [13].

Cerium oxide is well known for its ability to interact with molecular hydrogen [14]. It has a fluorite crystal structure (CaF_2), consisting of a cubic close-packed array of metal atoms with all tetrahedral holes filled by oxygen atoms. Each Ce^{4+} cation is surrounded by eight O^{2-} ions, which form the corners of a cube coordination. Each O^{2-} ion is surrounded by four cations in tetrahedron coordination. The interaction with hydrogen can be reversible [15,16] and it is spontaneous below 665 K [17]. Hydrogen insertion in ceria involves a progressive reduction of cerium cations [16,18–21] and its lattice expansion [22], with subsequent formation of OH groups [17].

The aim of this paper was to examine and describe the influence of cubic CeO_{2nano} as catalyst on hydrogen desorption from MgH_2, having in mind various factors mentioned above.

2. Experimental details

The commercial (Alfa Aeser) MgH_2 powder (AA) and CeO_2, synthesized by sol gel procedure in our laboratory [23], were used as starting materials. Ball milling process was performed under argon atmosphere for 10 h in Turbula Type 2TC Mixer using hardened steel vial and balls with BPR fixed at 10:1. Morphological and microanalytical characterization was carried out by VEGA TS 5130MM, Tescan Brno SEM equipped with EDS detector. XRD analysis was carried out on Siemens KRISTALLOFLEX D-500, with Cu-Kα Ni filtrated radiation (λ = 1.5406 Å). The diffracted X-rays were collected over 2θ range 10–90° using a step width of 0.02° with measuring time of 1 s per step. Since the Bragg peak broadening in XRD pattern is due to a combination of grain refinement (nanograin/crystallite) and lattice strain effects, it is common use to separate these two contributions by means of computation techniques. The separation of crystallite size and strain was obtained from Cauchy/Gaussian approximation by the linear regression plot according to the following equation:

$$\frac{\delta^2(2\theta)}{\tan^2\theta} = \frac{k\lambda}{L}\left(\frac{\delta(2\theta)}{\tan\theta\sin\theta}\right) + 16e^2 \tag{2}$$

where the term $k\lambda/L$ is the slope, the parameter L is the mean dimension of the nanograin (crystallite) composing the powder particle, k is constant (∼1) and e is the so-called ''maximum'' microstrain (calculated from the intercept), λ is the wave length and θ is the position of the analyzed peak maximum. Malvern 2000SM Mastersizer laser scattering particle size analysis system was used to obtain the quantitative MgH_2 particle size distributions. The specified resolution range of the system was sub-mm to 2 mm. 2-Propanol was used as suspension media. All samples were ultrasonicated for 15 min prior to measurements. All measurements were performed in the same stirring speed and obscuration level. Desorption properties of obtained MgH_2–CeO_2 composites were followed by TPD measurements at different heating rates ranging from 5 K/min to 25 K/min, starting from room temperature to 973 K, under initial vacuum of 3×10^{-6} mbar, utilizing homemade equipment with a quadruple mass spectrometer EXTORR XT300.

3. Results and discussion

X-ray diffractograms of commercial MgH_2 (AA) and milled composite MgH_2–CeO_2 are presented in Fig. 1. It can be seen that the mechanical milling of MgH_2 with CeO_2 led to broadening of typical β-MgH_2 peaks (β-MgH_2 has tetragonal structure, space group P4/2mnm), $2\theta = 28.1°$ (1 1 0), 35.96° (1 0 1), 40.1° (2 0 0). This is the result of crystallites size reduction and increase of microstrain. Crystallite size from

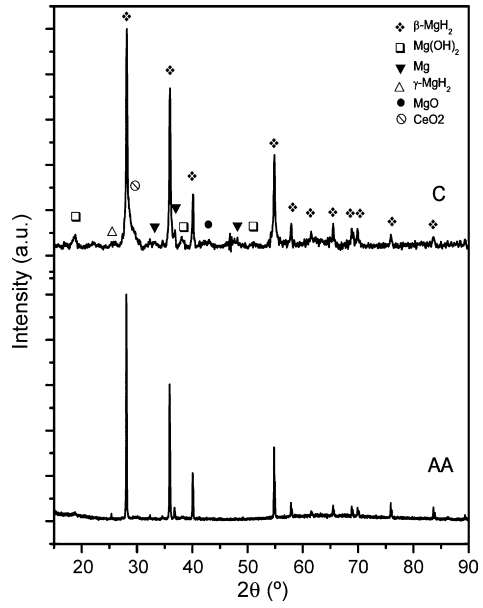

Fig. 1. XRD patterns of MgH_2 powder milled with 5 wt% of CeO_2 (C) and pure MgH_2 (AA).

83 nm for commercial MgH_2 was reduced to 36 nm for the composite, while the value for the microstrain was increased from 2.949×10^{-4} to 3.919×10^{4}. The XRD pattern also reveals additional peaks corresponding to CeO_2 at $2\theta = 33.20^{\circ}$, 47.60°, metallic Mg at $2\theta = 32.17^{\circ}$, MgO at $2\theta = 42.82^{\circ}$, $Mg(OH)_2$ at $2\theta = 18.44^{\circ}$ and 38.10°, and minor peaks assigned to γ-MgH_2.

Scanning electron micrographs of MgH_2–CeO_2 composite after ball milling are presented in Fig. 2. The composite has irregular shape agglomerates with sponge like structure ranging from 1 to 10 μm. Particle size distribution (PSD) of obtained composite has monomodal distribution with maximum at 4 μm (Fig. 3). At first glance, the results of SEM and PSD analysis seem to be contradictory, but one should have in mind the fact

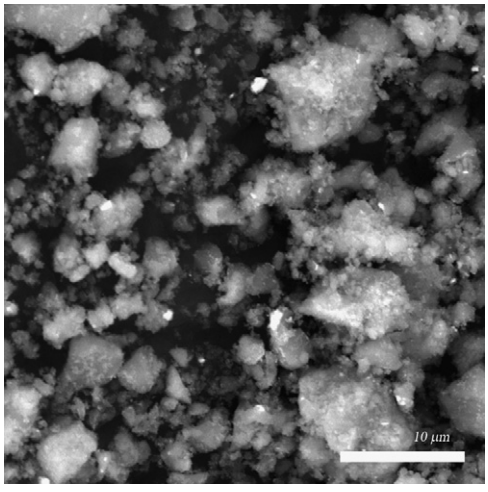

Fig. 2. Morphology of MgH_2–CeO_2 composites obtained by SEM BSE technique.

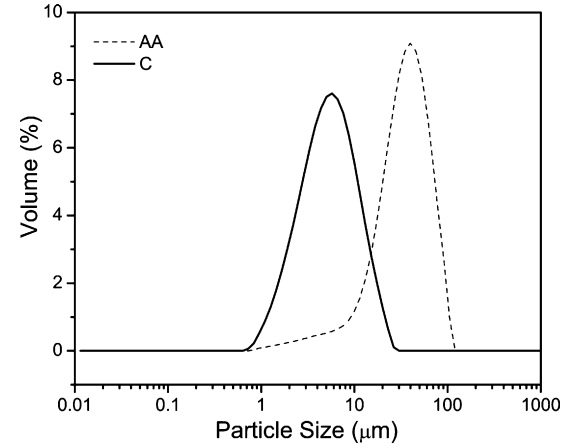

Fig. 3. Particle size distribution for MgH_2–CeO_2 composite (C) and non treated MgH_2 (AA).

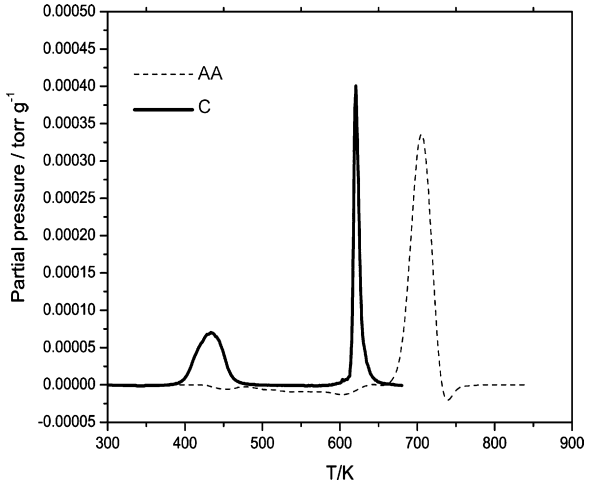

Fig. 4. TPD spectra of pure MgH_2 (AA) and MgH_2–CeO_2 composites (C) obtained with heating rate 5 K/min.

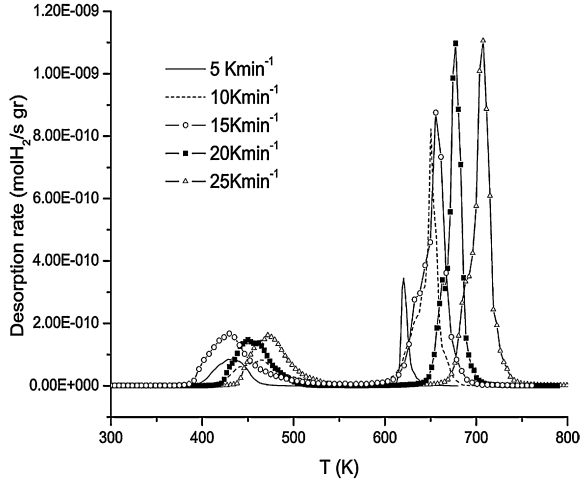

Fig. 5. H-desorption rate curves for MgH_2–CeO_2 at different heating rates. 5 K/min (solid line) 10 K/min (dash line), 15 K/min (empty circle), 20 K/min (filled square), 25 K/min (empty triangle).

that PSD analysis was done in constant ultrasound regime since the particles tends to agglomerate.

Results of TPD measurements are presented in Figs. 4 and 5. The starting material almost completely releases hydrogen in the single process around 706 K (Fig. 4). Two desorption maxima are visible for composite sample. The high temperature peak (HT) is positioned at 619 K while the low temperature peak was observed at 431 K (Fig. 4). It was found that the low-temperature peak (LT) originates from decomposition of $Mg(OH)_2$ while high temperature peak originate from H_2 [24,25]. Appearance of multiple peaks in TPD spectra could be related also to existence of both nanoparticles and coarse particles in the MgH_2–CeO_2 system, in accordance with literature data [26,27]. Anyhow, monomodal particle size distribution (by volume) is contradictory to this presumption, but one must have in mind that the fact that the particles have a tendency to agglomerate. The agglomerates of different sizes are visible in SEM figures (see Fig. 2). Fig. 5 shows TPD profiles at several heating rates, ranging from 5 K/min to 25 K/min as a function of temperature. Temperatures of HT maxima in relation to corresponding heating rates are given in Table 1.

The HT maxima shift to higher values when the heating rate increases from 5 K/min to 25 K/min. On the other hand, LT peaks do not follow linear dependence. This could be explained by the fact that hydrogen in LT peak comes from reactions of $Mg(OH)_2$ decomposition. According to results of DFT calculations done by Chafi et al., the existence of hydroxide can be explained by the reaction of one H atom and two O atoms coming from CeO_2. They demonstrated that (1 1 0) CeO_2 surface is particularly reactive, adsorbing easily H which penetrates below the surface without energy consumption [28]. When H-desorption occurs, the Mg–H bond of MgH_2 is triggered by the catalyst, in such way that the electrons of MgH_2 bonding orbitals are donated to the unoccupied orbitals of the catalyst, accompanied by a back-donation from the electrons of the occupied orbitals of the catalyst to the anti-bonding orbitals of MgH_2. This electronic exchange reaction has a consequence in easier Mg–H dissociation and therefore the accelerating recombination of hydrogen atoms.

The activation energy for the hydrogen desorption reaction, E_A^{des} was obtained from TPD measurements at different heating rates using Kissinger equation [13]. The E_A^{des} values were determined from the slope of the plot $\ln(\beta/T_p^2) = f(1/T_p)$. The obtained E_A^{des}, together with other literature data, is given in Table 2. The value of $E_A^{\mathrm{des}} = 60 \pm 10\,\mathrm{kJ/mol}$ for composite indicates that the activation energy of hydrogen desorption is sufficiently decreased by the catalytic effect of CeO_2 [29], so the surface activation of sample plays an important role in HD reaction [30]. Hanada et al. found the activation energies for catalyzed (MgH_2–Ni_{nano}) to be 94 + 3 kJ/mol H_2 and 323 + 40 kJ/mol H_2 for non catalyzed (MgH_2) samples [11]. Further, they have shown that the activation energy of surface activation process on the MgH_2 surface in the HD reaction is about 230 kJ/mol, indicating that the catalytic effect due to Ni_{nano}-doping significantly decreases the activation energy for hydrogen desorption by surface activation. Other authors has observe that the activation energy varies exponentially with the oxide content and reaches a limit of 62 kJ/mol at 0.2 mol% of oxide [31]. Consenquently, the rate-limiting step of the desorption has been changed from 'surface-controlled' to 'interface-controlled'. Taking into account pure MgH_2, Fernandez and Sanchez have determined the activation energy of the HD process [32]. They obtained the activation energy of 161 kJ/mol H_2. The observed disagreement in E_A^{des} for HD reaction of pure MgH_2 may be due to the difference between the used models. If one adopts the first-order reaction model without considering surface activation process, the activation energy is deduced to be as low as160 kJ/mol H_2. Lu et al. calculated the activation energy for dehydrogenation of MgH_2 in MgH_2 −0.1 mol.% cubic TiH_2 to be 58.4 kJ/mol H_2 [33]. This value is very close to the value obtained in our work. As we mentioned in the introduction, observed improvement in hydrogen desorption kinetics can be explained in terms of nonstoichiometric and/or vacant structure of CeO_2 after exposure to the hydrogen during desorption. The primary defects of concern are oxygen vacancies and small polarons (electrons localized on cerium cations). In case of oxygen defects, the increased diffusion rate of oxygen in the lattice causes increased catalytic activity. Borgschulte et al. investigated desorption properties of MgH_2 covered by the dissociated and recombined hydrogen during absorption/desorption at the oxide surface, as a function of vacancies formation [34]. According to DFT calculation performed by Du et al. the diffusion of H-vacancy from an in-plane site to a bridge site on the surface has the smallest activation barrier of 0.15 eV and should be fast at room temperature [35]. The calculated activation barriers for H-vacancy diffusion from the surface into sublayers are all less than 0.70 eV and are much smaller than the activation energy for desorption of hydrogen at the MgH_2 (1 1 0) surface (1.78–2.80 eV/H_2). This suggests that surface desorption is more likely than vacancy diffusion to be rate determining. Therefore, finding the effective catalyst on the

Table 1
Heat rate and T_{max} for both H desorption maxima in composite sample.

β(K/min)	T_{max}(HT) (K)	T_{max} (LT) (K)
5	619	431
10	650	465
15	655	429
20	677	456
25	706	473

Table 2
Activation energy E_A^{des} obtain in literature compared with our results.

Refs.	Composite	E_A^{des}(kJ/mol H_2)
[11]	MgH_2–Ni_{nano}	94 ± 3
[27]	$MgH_2/Mg(OH)_2$ mole fractions lower than 0.1 mole	167 ± 15
[29]	MgH_2–Nb_2O_5	71 ± 3
[31]	MgH_2–0.2 mol Nb_2O_5	62
[32]	Pure MgH_2	161 ± 15
[33]	MgH_2–0.1 mol.% cubic TiH_2	58.4
[37]	MgH_2–Ni/Ti (Ni/Ti) 4:1	81 ± 2.5
This study	MgH_2–CeO_2 cubic	60 ± 10

MgH_2 surface to facilitate desorption is very important for improving overall dehydrogenation performance. Obtained activation energy of 60 KJ/mol (0.63 eV) in case of MgH_2 catalyzed by CeO_2 supports the previous observations. Due to CeO_2 fluorite structure, the oxygen atoms in the ceria crystal are positioned in same the crystallographic plane, thus allowing rapid diffusion as a function of the number of oxygen vacancies. Mechanical milling increases the number of vacancies and easiness of oxygen movement in the crystal lattice, allowing the ceria to reduce and oxidize molecules or co-catalysts on its surface. So, the catalytic activity of ceria is directly related to the number of oxygen vacancies in the crystal [36]. According to Oelerich et al. oxides in which metal can have different valences have a superior catalytic effect, so the ability of the metal atom to take different electronic states could play an important role with respect to the kinetics of the solid–gas-reaction [2,3]. The influence of defects on the desorption properties has been resolved by Henrich. They have shown that (almost) perfect TiO_2 single-crystal surfaces are inert towards reactions with H_2, while H_2 is absorbed by TiO_2 surfaces that contain a higher density of defects in their crystal structure and thus also in the electronic surface structure [36]. Accordingly, the fast sorption kinetics of nanocrystalline MgH_2–CeO_2 systems may originate from a very high defect density, introduced at the surface of the metal oxide particles during high-energy ball milling [1,26,34].

4. Conclusion

The hydrogen desorption (HD) properties of the catalyzed MgH_2–CeO_2 composite prepared by mechanically milling the mixture of MgH_2 and cubic CeO_{2nano} has been investigated by means of TPD and Kissinger equation. The obtained value of the activation energy ($E_A^{des} = 60 \pm 10\,kJ/mol$) indicates that of hydrogen desorption is sufficiently decreased by the catalytic effect of CeO_2, so the surface activation of sample plays a major role in HD reaction. Morphology and microstructure of the samples were examined by XRD, SEM and particle size distribution and correlated with desorption properties. Significant improvement can be ascribed to the vacant CeO_2 structure.

Acknowledgment

This work was supported by the Serbian Ministry of Education and Science under grant III 45012.

References

[1] R.A. Varin, T. Czujko, Z.S. Wronski, Nanomaterials for Solid State Hydrogen Storage, first ed., Springer Science + Business Media, New York, 2009.
[2] W. Oelerich, T. Klassen, R. Bormann, Metal oxides as catalysts for improved hydrogen sorption in nanocrystalline Mg-based materials, J. Alloys Compd. 315 (2001) 237–242.
[3] W. Oelerich, T. Klassen, R. Bormann, Comparison of the catalytic effects of V, V_2O_5, VN, and VC on the hydrogen sorption of nanocrystalline Mg, J. Alloys Compd. 322 (2001) L5–L9.
[4] N. Hanada, T. Ichikawa, S. Isobe, T. Nakagawa, K. Tokoyoda, T. Honma, H. Fujii, Y. Kojima, X-ray absorption spectroscopic study on valence state and local atomic structure of transition metal oxides doped in MgH_2, J. Phys. Chem. C 113 (2009) 13450–13455.
[5] A. Borgschulte, U. Bosenberg, G. Barkhordarian, M. Dornheim, R. Bormann, Enhanced hydrogen sorption kinetics of magnesium by destabilized $MgH_{2-\delta}$, Catal. Today 120 (3–4) (2007) 262–269.
[6] C.X. Shang, Z.X. Guo, Structural and desorption characterizations of milled (MgH_2 + Y, Ce) powder mixtures for hydrogen storage, Int. J. Hydrogen Energy 32 (14) (2007) 2920–2925.
[7] R. Janot, X. Darok, A. Rougier, L. Aymard, G.A. Nazrinn, J.-M. Tarascon, Hydrogen sorption properties for surface treated MgH_2 and Mg_2Ni alloys, J. Alloys Compd. 404–406 (2005) 293–296.
[8] M.Y. Song, J.-L. Bobet, B. Darriet, Improvement in hydrogen sorption properties of Mg by reactive mechanical grinding with Cr_2O_3, Al_2O_3 and CeO_2, J. Alloys Compd. 340 (1–2) (2002) 256–262.
[9] J. Huot, G. Liang, S. Boily, A. Van Neste, R.R. Schulz, Structural study and hydrogen sorption kinetics of ball-milled magnesium hydride, J. Alloys Compd. 293–295 (1999) 495–500.
[10] J.F. Fernandez, C.R. Sanchez, Rate determining step in the absorption and desorption of hydrogen by magnesium, J. Alloys Compd. 340 (2002) 189–198.
[11] N. Hanada, T. Ichikawa, H. Fujii, Catalytic effect of nanoparticle 3d-transition metals on hydrogen storage properties in magnesium hydride MgH_2 prepared by mechanical milling, J. Phys. Chem. B 109 (15) (2005) 7188–7194.
[12] L. Schlapbach (Ed.), Hydrogen in Intermetallic Compounds 2, Springer-Verlag, Berlin, 1992, p. 69.
[13] H.E. Kissinger, Reaction kinetics in differential thermal analysis, Anal. Chem. 29 (1957) 1702–1706.
[14] A. Trovarelli, Catalytic properties of ceria and CeO_2-contaning materials, Cat. Rev. – Sci. Eng. 38 (4) (1996) 439–520.
[15] J. Bernal, J.J. Calvino, G.A. Cifredo, J.M. Gatica, J.A. Perez Omil, J.M. Pintado, Hydrogen chemisorption on ceria: influence of the oxide surface area and degree of reduction, J. Chem. Soc. Faraday Trans. 89 (18) (1993) 3499–3505.
[16] A. Bensalem, F. Bozonverduraz, V. Perrichon, Palladium-ceria catalysts: reversibility of hydrogen chemisorption and redox phenomena, J. Chem. Soc. Faraday Trans. 91 (14) (1995) 2185–2189.
[17] K. Sohlberg, S.T. Pantelides, S.J. Pennycook, Interactions of hydrogen with CeO_2, J. Am. Chem. Soc. 123 (27) (2001) 6609–6611.
[18] J.L.G. Fierro, J. Soria, J. Sanz, J.J.M. Rojo, Temperature-programmed desorption study of the interactions of H_2, CO and CO_2 with $LaMnO_3$, J. Solid State Chem. 66 (1987) 154–162.
[19] A. Laachier, V. Perrichon, A. Vadri, L. Lamotte, E. Catherine, J.C. Lavalley, J. El Fallah, L. Hilaire, F. Normand, E. Quemere, G.N. Sauvion, O. Touret, Reduction of CeO_2 by hydrogen. Magnetic susceptibility and Fourier-transform infrared, ultraviolet and X-ray photoelectron spectroscopy measurements, J. Chem. Soc. Faraday Trans. 87 (10) (1991) 1601–1609.
[20] S. Yamanaka, T. Nishizaki, M. Uno, M. Katsura, Hydrogen dissolution into zirconium oxide, J. Alloys Compd. 293–295 (1999) 38–41.
[21] M. Miyake, M. Uno, S. Yamanaka, On the zirconium–oxygen–hydrogen ternary system, J. Nucl. Mater. 270 (1999) 233–241.
[22] C. Lamonier, G. Wrobel, J.P. Bonnelle, Behaviour of ceria under hydrogen treatment: thermogravimetry and in situ X-ray diffraction study, J. Mater. Chem. 4 (1994) 1927–1928.
[23] J.J. Gulicovski, S.K. Milonjić, K. Mészáros Szécsényi, Synthesis and characterization of stable aqueous ceria sols, Mater. Manuf. Processes 24 (10) (2009) 1080–1085.
[24] S. Kurko, Ž. Rašković, N. Novaković, B. Paskaš Mamula, Z. Jovanović, Z. Baščarević, J. Grbovic Novaković, Lj. Matović, Hydrogen storage properties of MgH_2 mechanically milled with α and β SiC, Int. J. Hydrogen Energy 36 (1) (2011) 549–554.
[25] F. Leardini, J.R. Ares, J. Bodega, J.F. Fernandez, I.J. Ferrer, C. Sanchez, Reaction pathways for hydrogen desorption from magnesium hydride/hydroxide composites: bulk and interface effects, Phys. Chem. Chem. Phys. 12 (2010) 572–577.
[26] R.A. Varin, T. Czujko, Ch. Chiu, Z. Wronski, Particle size, grain size and γ-MgH_2 effects on the desorption properties of nanocrystalline commer-

cial magnesium hydride processed by controlled mechanical milling, Nanotechnology 17 (2006) 3856–3865.
[27] A. Bassetti, E. Bonetti, L. Pasquini, A. Montone, J. Grbović, M. Vittori Antisari, Hydrogen desorption from ball milled MgH_2 catalyzed with Fe, Eur. Polym. J. 43 (2005) 19–37.
[28] Z. Chafi, N. Keghouche, C. Minot, Density function theoretical study of interaction of hydrogen with ceria, Phys. Procedia 2 (3) (2009) 673–676.
[29] N. Hanada, T. Ichikawa, S. Hino, H. Fuji, Remarkable improvement of hydrogen sorption kinetics in magnesium catalyzed with Nb_2O_5, J. Alloys Compd. 420 (1–2) (2006) 46–49.
[30] J. Grbović Novaković, Lj. Matović, M. Drvendžija, N. Novaković, D. Rajnović, M. Šiljegović, Z. Kačarević-Popović, S. Milovanović, N. Ivanović, Changes of hydrogen storage properties of MgH_2 induced by heavy ion irradiation, Int. J. Hydrogen Energy 33 (7) (2008) 1876–1879.
[31] G. Barkhordarian, T. Klassen, R. Bormann, Effect of Nb_2O_5 content on hydrogen reaction kinetics of Mg, J. Alloys Compd. 364 (1–2) (2004) 242–246.
[32] J.F. Fernandez, C.R. Sanchez, Simultaneous TDS–DSC measurements in magnesium hydride, J. Alloys Compd. 356–357 (2003) 348–352.
[33] J. Lu, Y.J. Choi, Z. Zak Fang, Hydrogen storage properties of nanosized MgH_2–$0.1TiH_2$ prepared by ultrahigh-energy-high-pressure milling, J. Am. Chem. Soc. 131 (2009) 15843–15852.
[34] A. Borgschulte, M. Bielmann, A. Zuttel, G. Barkhordarian, M. Dornheim, R. Bormann, Hydrogen dissociation on oxide covered MgH_2 by catalytically active vacancies, Appl. Surf. Sci. 254 (2008) 2377–2384.
[35] A.J. Du, S.C. Smith, G.Q. Lu, First-principle studies of the formation and diffusion of hydrogen vacancies in magnesium hydride, J. Phys. Chem. C 111 (23) (2007) 8360–8365.
[36] V. Henrich, The surfaces of metal oxides, Rep. Prog. Phys. 48 (11) (1985) 1481–1541.
[37] H.B. Lu, C.K. Poh, L.C. Zhang, Z.P. Guo, X.B. Yu, H.K. Liu, Dehydrogenation characteristics of Ti- and Ni/Ti-catalyzed Mg hydrides, J. Alloys Compd. 481 (1–2) (2009) 152–155.